Synthesis and Characterization of Three New Layered Phosphates, $Na_2MnP_2O_7$, $NaCsMnP_2O_7$, and $NaCsMn_{0.35}Cu_{0.65}P_2O_7$

Qun Huang and Shiou-Jyh Hwu*

Department of Chemistry and Materials Science & Engineering Program, Clemson University, Clemson, South Carolina 29634-1905

Received June 2, 1998

Three new layered phosphates were isolated by employing high-temperature, solid-state reactions. These compounds belong to the $A^I_2B^{II}P_2O_7$ family. $Na_2MnP_2O_7$, **1**, crystallizes in the triclinic space group $P\bar{1}$ (No. 2) with a = 5.316(2) Å, b = 6.580(2) Å, c = 9.409(3) Å, α = 109.65(3)°, β = 95.25(3)°, γ = 106.38(3)°, and Z = 2; $NaCsMnP_2O_7$, **2**, crystallizes in the orthorhombic space group $Cmc2_1$ (No. 36) with a = 5.332(2) Å, b = 15.009(2) Å, c = 9.808(2) Å, and Z = 4; $NaCsMn_{0.35}Cs_{0.65}P_2O_7$, **3**, also crystallizes in the orthorhombic space group $Cmc2_1$ (No. 36) with a = 5.208(2) Å, b = 15.073(5) Å, c = 9.708(3) Å, and Z = 4. **1** possesses a new structure type composed of slabs of fused $Mn_4P_4O_{26}$ cages, and **2** and **3** are isostructural with $K_2CuP_2O_7$. The unique cage structure found in **1** is made of two edge-sharing Mn_2O_{10} dimers and two P_2O_7 pyrophosphate groups. These units, arranged in parallel with respect to Mn−Mn and P−P vectors, are linked in an alternating fashion through corner-sharing oxygen atoms. Incorporation of larger Cs^+ cations leads to a different structure in **2** and **3**, while substituting similarly sized Cu^{2+} for Mn^{2+} cations in **3** does not alter the structure type. Magnetic susceptibility measurements as well as bond valence sum calculations confirm the valence states of cations, including the high-spin, d^5 Mn^{2+} cation. UV−vis and IR spectra of **1** and **2** are presented. In this report, the discrete nature of the manganese oxide lattices is discussed.

Introduction

Transition metal−oxide (TM−oxide) chemistry involving closed-shell, nonmagnetic silicate, phosphate, and arsenate oxyanions has attracted much attention because of their varied framework structures. The interest is more in the properties of structurally confined TM−oxide frameworks, not really in size.[1,2] The tetrahedrally coordinated oxyanions behave like chelating agents with respect to TM−oxide layers, chains, and oligomers. Studies have shown that d electrons in nanostructured TM−oxide lattices are confined. For example, Nakua and Greedan showed no short-range magnetic ordering between isolated M^{2+} magnetic centers in three transition metal arsenates MAs_2O_6 (M = Mn, Co, Ni).[3] They reported that the absence of significant short-range coupling is due to the absence of a superexchange M−O−M pathway. The dominant M−O−X−O−M linkage disrupts the electron interaction between M^{m+} cations because of the closed-shell X^{n+} ions (Si^{4+}, P^{5+}, As^{5+}). In $BaTi_2(P_2O_7)_2$, we have shown similar magnetic behavior where the Ti^{3+} d^1 electron acts like that in a discrete molecule.[4]

The structural chemistry of this compound class is extremely rich. New phases are often discovered by changing target composition, reaction temperature, redox chemistry, and reaction media. In recent studies of the A−Mn−P−O systems, three new phases of the $A^I_2B^{II}X_2O_7$ type (A = monovalent metal cations; B = divalent transition metal cations) have been isolated. Prior to this study, several TM-containing compounds of this class have been reported, e.g., $A_2CuP_2O_7$ (A = Li, Na, K),[5] $A_2MP_2O_7$ (A = Na, K; M = Co, Zn),[6] $K_2NiP_2O_7$,[7] $K_2CdP_2O_7$,[8] $K_2MnP_2O_7$,[9] and $A_2PdP_2O_7$ (A = Li, Na).[10] In this paper, the syntheses and characterization of $Na_2MnP_2O_7$, **1**, $NaCsMnP_2O_7$, **2**, and $NaCsMn_{0.35}Cu_{0.65}P_2O_7$, **3**, are discussed. **1** exhibits a novel structure type; **2** and **3** are isostructural with $K_2CuP_2O_7$.[5c] Both UV−vis spectroscopy and magnetic susceptibility results are also presented.

* To whom correspondence should be addressed at the Department of Chemistry.

(1) Hwu, S.-J. *Chem. Mater.*, in press.
(2) (a) Wang, S.; Hwu, S.-J. *J. Am. Chem. Soc.* **1992**, *114*, 6920. (b) Serra, D. L.; Hwu, S.-J. *J. Solid State Chem.* **1992**, *101*, 32. (c) Wang, S.; Hwu, S.-J. *Inorg. Chem.* **1995**, *34*, 166. (d) Wang, S.; Hwu, S.-J.; Paradis, J. A.; Whangbo, M.-H. *J. Am. Chem. Soc.* **1995**, *117*, 5515. (e) Etheredge, K. M. S.; Hwu, S.-J. *Inorg. Chem.* **1995**, *34*, 5013. (f) Etheredge, K. M. S.; Hwu, S.-J. *Inorg. Chem.* **1996**, *35*, 5278. (g) Mackay, T.; Wardojo, T. A.; Hwu, S.-J. *J. Solid State Chem.* **1996**, *125*, 255. (h) Hase, M.; Etheredge, K. M. S.; Hwu, S.-J.; Shirane, G. *Phys. Rev. B* **1997**, *56*, 3231.
(3) Nakua, A. M.; Greedan, J. E. *J. Solid State Chem.* **1995**, *118*, 402.
(4) (a) Wang, S.; Hwu, S.-J. *J. Solid State Chem.* **1991**, *90*, 31. (b) Wang, S. Ph.D. Dissertation, Rice University, 1993.
(5) (a) $Li_2CuP_2O_7$: Spirlet, M. R.; Rebizant, J.; Liegeois-Duyckaerts, M. *Acta Crystallogr.* **1993**, *C49*, 209. (b) $Na_2CuP_2O_7$: Etheredge, K. M. S.; Hwu, S.-J. *Inorg. Chem.* **1995**, *34*, 1495. (c) $K_2CuP_2O_7$: ElMaadi, A.; Boukhari, A.; Holt, E. M. *J. Solid State Chem.* **1995**, *223*, 13.
(6) (a) $Na_2CoP_2O_7$, $P\bar{1}$, $P2_1cn$: Erragh, F.; Boukhari, A.; Elouadi, B.; Holt, E. M. *J. Cryst. Spectrosc. Res.* **1991**, *21*, 321. (b) $A_2MP_2O_7$ (A = Na, K.; M = Co, Zn): Gabélica-Robert, M. *C. R. Acad. Sci., Ser. II* **1981**, *293*, 497.
(7) $K_2NiP_2O_7$: Elmaadi, A.; Boukhari, A.; Holt, E. M. *J. Chem. Crystallogr.* **1995**, *25*, 531.
(8) $K_2CdP_2O_7$: Faggiani, R.; Calvo, C. *Can. J. Chem.* **1976**, *54*, 3319.
(9) $K_2MnP_2O_7$: Elmaadi, A.; Boukhari, A.; Holt, E. M.; Flandrois, S. *C. R. Acad. Sci., Ser. II* **1994**, *318*, 765.
(10) (a) $Li_2PdP_2O_7$: Laligant, Y. *Eur. J. Solid State Inorg. Chem.* **1992**, *29*, 239. (b) $Na_2PdP_2O_7$: Laligant, Y. *Eur. J. Solid State Inorg. Chem.* **1992**, *29*, 83.

10.1021/ic980616d CCC: $15.00
Published on Web 10/09/1998

Experimental Section

Synthesis. All chemicals were used as purchased (CuO, Strem, 99.999%; Na_2O, Alfa, 86%; MnO_2, Aldrich, 99+%; P_2O_5, Aldrich, 98+%; NaCl, Alfa, 99.99%, or Strem, 99.999%; CsCl, Aldrich, 99%). The reactions were performed in fused-silica ampules under vacuum.

(a) $Na_2MnP_2O_7$ (1). The reaction mixture of Na_2O (2.0 mmol), MnO_2 (2.0 mmol), and P_2O_5 (2.0 mmol) was heated to 600 °C over 24 h and held at that temperature for 48 h, followed by soaking for an additional 5 days at 750 °C. The reaction mixture was cooled slowly to 500 °C over 48 h, followed by furnace cooling over 20 h to room temperature by simply switching off the power. Colorless transparent crystals of **1** were obtained along with some purple-green phases, $Na_2Mn_3(PO_4)_3$.[11]

(b) $NaCsMnP_2O_7$ (2). This compound was isolated from a similar reaction where halide flux was employed. Na_2O (1.0 mmol), MnO_2 (1.0 mmol), and P_2O_5 (1.0 mmol) were ground and mixed with the eutectic flux NaCl/CsCl (67:33 mol %, mp = 493 °C). The flux-to-charge ratio was 5:1. The reaction was performed in a carbon-coated fused-silica ampule as described elsewhere.[2] The mixture was heated to 500 °C over 19 h and held at that temperature for 48 h, followed by soaking for 5 days at 700 °C. The reaction mixture was first slowly cooled to 400 °C over 4 days and then furnace-cooled to room temperature. Purple column crystals of **2** as well as some dark-red crystals of $CsNa_3Mn_7(PO_4)_6$[11] were retrieved from the flux by washing the products with deionized water using suction filtration. Compound **2** is slightly moisture-sensitive and gradually decomposes in air.

(c) $NaCsCu_{0.65}Mn_{0.35}P_2O_7$ (3). $KMnO_4$ (1.0 mmol), CuO (1.0 mmol), and P_2O_5 (1.0 mmol) were mixed and ground with the eutectic flux NaCl/CsCl (67:33 mol %; mp = 493 °C). The flux-to-charge ratio was 5:1. The reaction was also performed in a carbon-coated fused-silica ampule. The mixture was heated to 500 °C over 19 h and held at that temperature for 48 h, followed by soaking for 2 days at 700 °C. The reaction mixture was first slowly cooled to 400 °C over 4 days and then furnace-cooled to room temperature. Light-orange crystals of **3** as well as some dark-red crystals of $CsNa_3(Mn,Cu)_7(PO_4)_6$[11] and some pinkish crystals of unidentified composition were retrieved upon washing with deionized water and suction filtration. EDAX showed the presence of Mn and Cu and, remarkably, no K in **3**. Compound **3** is somewhat moisture-sensitive and decomposes to a light blue crystalline powder after extensive exposure to air.

Single-Crystal X-ray Diffraction. Crystals of **1** (0.18 × 0.16 × 0.11 mm), **2** (0.12 × 0.17 × 0.44 mm), and **3** (0.24 × 0.19 × 0.13 mm) were selected and mounted on glass fibers for X-ray single-crystal diffraction analyses. The crystallographic data are given in Table 1. The diffraction data were collected on a Siemens R3m/v diffractometer (Mo Kα, λ = 0.710 73 Å) equipped with a graphite monochromator. Unit cell constants were obtained on the basis of least-squares fits of up to 50 reflections. No detectable decay was observed during the data collection, judging from the intensities of three standard reflections which were measured every 100 reflections. Lorentz−polarization and empirical absorption corrections[12] (ψ scans) were applied to the data.

The structures were solved by direct methods with SHELXS-86[13] and refined on $|F|$ with SHELXTL-Plus[14] by least-squares, full-matrix techniques.[15] The positions of the Mn, the P, and part of the oxygen atoms for **1** and of the Cs, the Mn(Cu), the P, and part of the oxygen atoms for **2** and **3** were obtained directly from the Fourier synthesis map. The remaining atoms were located from the difference Fourier maps. Except for the disordered oxygen atoms in **2**, all oxygen atoms were refined anisotropically. The secondary extinction factors were refined. Other possible space groups (*Cmcm* and *Ama*2) for **2** and **3** were checked. For **2** and **3**, redundant data were collected and Friedel pair analysis was performed to determine the correct enantiomorph. The atomic coordinates and equivalent thermal parameters are listed in Table 2.

Table 1. Crystallographic Data[a] for $Na_2MnP_2O_7$ (**1**), $NaCsMnP_2O_7$ (**2**), and $NaCsMn_{0.35}Cu_{0.65}P_2O_7$ (**3**)

	1	**2**	**3**
empirical formula	$Na_2MnP_2O_7$	$NaCsMnP_2O_7$	$NaCsMn_{0.35}Cu_{0.65}P_2O_7$
fw	274.9	384.8	390.4
space group	$P\bar{1}$ (No. 2)	$Cmc2_1$ (No. 36)	$Cmc2_1$ (No. 36)
a, Å	5.316(2)	5.332(2)	5.208(2)
b, Å	6.580(2)	15.009(2)	15.073(5)
c, Å	9.409(3)	9.808(2)	9.708(3)
α, deg	109.65(3)		
β, deg	95.25(3)		
γ, deg	106.38(3)		
V, Å^3	290.96(17)	784.9(4)	762.1(5)
Z	2	4	4
T, °C	23	23	23
λ, Å	0.710 73	0.710 73	0.710 73
ρ_{calcd}, g cm^{-3}	3.137	3.256	3.402
linear abs coeff, mm^{-1}	2.955	6.708	7.647
$R(F_o)$,[b] %	2.29	2.25	2.14
$R_w(F_o)$,[c] %	4.08	2.98	2.96

[a] The cell constants are refined in each designated crystal system (**1**, 50 reflections, 28.69 < 2θ < 54.94°; **2**, 49 reflections, 31.19 < 2θ < 54.34°; **3**, 50 reflections, 30.15 < 2θ < 48.34°). [b] $R = \sum||F_o| - |F_c||/\sum|F_o|$. [c] $R_w = [\sum w(|F_o| - |F_c|)^2/\sum w|F_o|^2]^{1/2}$; $w = 1/[\sigma^2(F) + aF^2]$.

Infrared Spectroscopy. IR spectroscopy was performed using a Perkin-Elmer 1600 Series FTIR instrument over the range 1500−400 cm^{-1}. Sixteen scans were obtained at 2.0 cm^{-1} increments. The samples were prepared as KBr disks from the ground powder of selected crystals **1** and **2**.

UV−Vis Diffuse Reflectance Spectroscopy. Optical absorption spectra were obtained from a PC-controlled Shimadzu UV-3100 UV/vis/near-IR spectrometer equipped with an integrating sphere. $BaSO_4$ was used as a reflectance standard. UV−vis diffuse reflectance spectra of the title compounds were taken in the range of 200 nm (6.2 eV) to 2500 nm (0.50 eV). Data were collected in the reflectance (*R*%) mode and manually converted to arbitrary absorption units (α/s) by the relationship $A = \alpha/s = (1 - R/100)^2/2(R/100)$.[16]

Magnetic Measurements. The temperature-dependent magnetic susceptibilities of **1** and **2** were measured using a Quantum Design SQUID MPMS-5S magnetometer at field strength 0.5 T in the temperature ranges 1.84−300 K for **1** and 1.75−300 K for **2**. Ground selected single crystals (5.6 and 11.3 mg, respectively) were contained in gel capsule sample holders which were suspended in a straw from the sample translator drive. The temperature and field dependence of the susceptibility of the container were previously determined. The magnetic susceptibilities were corrected for the effect of gel capsule and for core diamagnetism with Pascal's constants.[17]

Results and Discussion

We are once again intrigued by the structural diversity of transition metal phosphate compounds. New phases have been isolated as a result of a slight change in reaction conditions. In the present studies, the compounds $Na_2MnP_2O_7$, **1**, and $NaCsMnP_2O_7$, **2**, were isolated from reactions using the same starting materials in the same molar ratios. For the synthesis of **1**, no flux was employed, while, in the synthesis of **2**, an NaCl/CsCl eutectic flux was used. While a halide flux aids crystal

(11) Huang, Q.; Hwu, S.-J. Clemson University. Unpublished research, 1997.
(12) North, A. C. T.; Phillips, D. C.; Mathews, F. S. *Acta Crystallogr.* **1968**, *A24*, 351.
(13) Sheldrick, G. M. In *Crystallographic Computing 3*; Sheldrick, G. M., Kruger, C., Goddard, R., Eds.; Oxford University Press: London, 1985; pp 175−189.
(14) Sheldrick, G. M. *SHELXTL-PLUS, Version 4.2.1 Structure Determination Software Programs*; Siemens Analytical X-ray Instruments Inc.: Madison, WI, 1990.
(15) Busing, W. R.; Martin, K. O.; Levy, H. A. *ORFLS*; Report ORNL-TM-305; Oak Ridge National Laboratory: Oak Ridge, TN, 1962.
(16) (a) Kubelka, P.; Munk, F. *Z. Tech. Phys.* **1931**, *12*, 593. (b) Kubelka, P. *J. Opt. Soc. Am.* **1948**, *38*, 448.
(17) O'Connor, C. J. *Prog. Inorg. Chem.* **1982**, *29*, 203.

Table 2. Atomic Coordinates ($\times 10^4$) and Equivalent Isotropic Displacement Coefficients, U_{eq} ($Å^2 \times 10^3$), for $Na_2MnP_2O_7$, $NaCsMnP_2O_7$, and $NaCsMn_{0.35}Cu_{0.65}P_2O_7$

atom	*x*	*y*	*z*	U_{eq}[a]
		$Na_2MnP_2O_7$		
Mn	881(1)	6003(1)	3628(1)	9(1)
P(1)	2579(1)	1630(1)	3887(1)	8(1)
P(2)	4331(1)	3312(1)	1346(1)	9(1)
Na(1)	−3485(2)	8680(2)	2718(1)	22(1)
Na(2)	1248(2)	−2223(2)	366(1)	31(1)
O(1)	668(3)	3009(3)	4203(2)	12(1)
O(2)	4888(3)	2398(3)	5195(2)	17(1)
O(3)	1023(3)	−910(3)	3308(2)	18(1)
O(4)	3744(4)	1833(3)	2422(2)	25(1)
O(5)	2680(3)	4904(3)	1674(2)	13(1)
O(6)	3366(4)	1522(3)	−260(2)	18(1)
O(7)	7301(3)	4546(3)	1789(2)	20(1)
		$NaCsMnP_2O_7$[b]		
Cs	0	4055(1)	7662(1)	25(1)
Na	5000	6402(2)	5982(4)	27(1)
Mn	0	3133(1)	3638	12(1)
P(1)	0	2198(1)	527(2)	13(1)
P(2)	5000	4409(1)	3923(2)	11(1)
O(1)	2699(8)	4099(3)	3148(5)	25(1)
O(2)	0	1122(4)	10371(6)	20(2)
O(3)	5000	5365(4)	4308(6)	27(2)
O(4)	−2551(18)	2483(6)	115(9)	19(1)
O(5)	−8018(18)	7389(6)	4597(11)	19
O(6)	0	2226(13)	2154(18)	18(2)
O(7)	837(34)	2408(9)	1908(14)	18
		$NaCsMn_{0.35}Cu_{0.65}P_2O_7$[c]		
Cs	0	5949(1)	2338	28(1)
Na	−5000	3573(2)	3948(3)	26(1)
Cu	0	6808(1)	6291(1)	16(1)
Mn	0	6808	6291	16
P(1)	0	7781(1)	9509(2)	19(1)
P(2)	−5000	5593(1)	6003(2)	14(1)
O(1)	0	8848(3)	−445(4)	25(1)
O(2)	−2401(11)	7485(3)	146(9)	76(3)
O(3)	−806(15)	7550(5)	8068(8)	49(3)
O(4)	2646(7)	5891(2)	6795(4)	28(1)
O(5)	−5000	4647(3)	5593(5)	34(2)

[a] Equivalent isotropic *U* defined as one-third of the trace of the orthogonalized $\mathbf{U}_{ij}$ tensor. [b] O(4) and O(5) are a disordered pair as well as O(6) and O(7). The sum of the occupancy for each pair is constrained to 1.0. The refined occupancies are 0.569(9), 0.431(9), 0.40(1), and 0.30(1) × 2. [c] Cu(1) and Mn(1) are disordered at the same position. The sum of their occupancies is constrained to 1.0. The refined occupancies are 0.65(1) and 0.35(1), respectively. O(3) is disordered around a 2-fold axis, and its occupancy is fixed at 0.5.

growth, incorporation of the electropositive cations from the fluxes employed is inevitable. Crystals of $NaCsCu_{0.65}Mn_{0.35}P_2O_7$, **3**, were obtained in a continued effort to synthesize high oxidation state Mn phases[18] by employing potassium permanganate. Due to the acidic environment, $KMnO_4$ decomposes to lower-valent manganese oxides, resulting in a low yield **3**.

The incorporated A-site cations play an important role in the framework formation. In the present series, $Na_2MnP_2O_7$ forms a new structure type, while $NaCsMnP_2O_7$ and $NaCsCu_{0.65}Mn_{0.35}P_2O_7$ adopt the $K_2CuP_2O_7$ structure.[5c] The difference in structures is attributed to the inclusion of the large Cs^+ cation. This size effect is observed in the previously studied $A_2CuP_2O_7$ (A = Li, Na, K) family.[5] Both Li and Na phases form undulating $[CuP_2O_7]_\infty$ ribbons, and the K compound exhibits undulating $[CuP_2O_7]_\infty$ slabs. The A-site cations reside in the gap between stacked ribbons and slabs, and different unit cells are formed

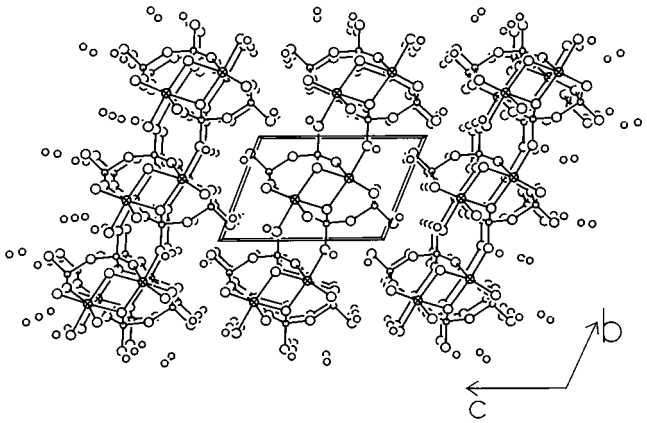

Figure 1. Perspective view of $Na_2MnP_2O_7$ along the *a* axis. The unit cell is outlined. The large crosshatched and small open circles represent Mn and P, respectively, and the large open circles are O. The unbounded small circles represent Na.

to accommodate the coordination geometry of AO_n, where $n = 4-9$. In the $A_2MnP_2O_7$ (A = Na, K) series, however, the two unit cells are distinctly different. The $Na_2MnP_2O_7$ compound possesses edge-shared Mn_2O_{10} dimers (see below), and the $K_2MnP_2O_7$ phase contains an isolated MnO_6 octahedron. The Na^+ cations adopt 7- or 8-coordination in the presently studied $Na_2MnP_2O_7$, and K^+ cations possesses a higher (8- or 9-) coordination in $K_2MnP_2O_7$.[9] The average Na−O distance is in a range of 2.58−2.63 Å, and the K−O distance is between 2.88 and 2.89 Å. Substituting Cu^{2+} for Mn^{2+} does not alter the structure type seemingly because these cations are similar in size, 0.87 Å vs 0.81 Å for 6-coordinate, divalent cations, respectively.[19]

Compound **1** crystallizes in the triclinic space group $P\bar{1}$, and it adopts a new structure type consisting of a fascinating $Mn_4P_4O_{26}$ cage. Figure 1 shows the packing diagram with the unit cell outlined. This extended framework is composed of two-dimensional Mn−P−O slabs with Na^+ cations residing between the parallel slabs. The Mn−P−O slab is made of corner-shared structural units of Mn_2O_{10} dimers and P_2O_7 groups. Two Mn_2O_{10} dimers and two pyrophosphate groups are alternately arranged such that the Mn−Mn and P−P vectors are parallel, and roughly along ⟨011⟩, in the formation of the $Mn_4P_4O_{26}$ cage. Through sharing opposite dimers, the cages are fused together to form a chain extended along the *a* axis. Figure 2 shows a partial structure of the chain which contains two cages sharing a common Mn_2O_{10} dimer. The parallel chains are interlinked by sharing O(3) atoms to form the Mn−P−O slab. The unshared oxygen atom O(6) pointing into the gap forms the shortest Na−O bond, 2.279(2) Å. Each Mn atom is 6-coordinate with oxygen atoms from four P_2O_7 groups in a distorted octahedral geometry. The Mn−Mn distance in the edge-shared dimer is 3.365(2) Å, and the Mn−O(1)−Mn angle is 99.1(1)°. The average Mn−O bond length is 2.18 Å, which is comparable to the distance of 2.20 Å observed in $K_2MnP_2O_7$,[9] where the MnO_6 octahedron also displays a distorted configuration. For the P_2O_7 group, the P−O−P bond angle is 145.8°, the terminal P−O bond is 1.51 Å, and the bridging P−O bond is 1.61 Å, which are all comparable with those values in related compounds.

As stated above, compounds **2** and **3** are isostructural with $K_2CuP_2O_7$, which crystallizes in the orthorhombic space group $Cmc2_1$. The general features of the structure are represented in Figure 3. The corner-shared MnO_5 and P_2O_7 units are alternately

(18) For example, $Na_4Mn^{VII}_{0.5}P^{V}_{0.5}O_5$: Etheredge, K. M. S.; Gardberg, A. S.; Hwu, S.-J. *Inorg. Chem.* **1996**, *35*, 6358.

(19) Shannon, R. D. *Acta Crystallogr.* **1976**, *A32*, 751.

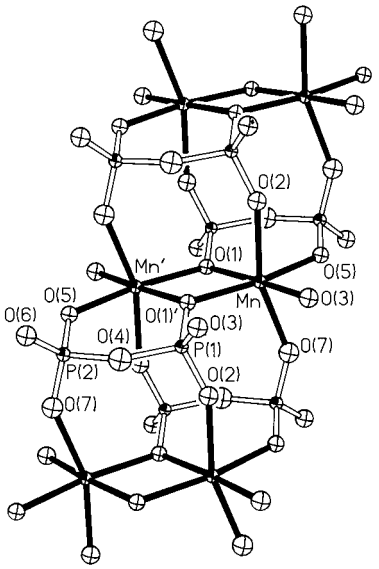

Figure 2. Two empty $Mn_4P_4O_{26}$ cages in $Na_2MnP_2O_7$ fused by sharing a common Mn_2O_{10} dimer. Each cage is centered by the inversion center. The Mn_2O_{10} dimer is highlighted by solid lines, and the P_2O_7 unit is outlined by hollow lines. The anisotropic thermal ellipsoids are drawn at 70% probability. (Mn−O(1) = 2.188(2) Å, Mn−O(1)′: 2.232(2) Å, Mn−O(2) = 2.195(2) Å, Mn−O(3) = 2.134(2) Å, Mn−O(5) = 2.153(2) Å, Mn−O(7) = 2.188(2) Å; P(1)−O(1)′: 1.529(2) Å, P(1)−O(2) = 1.494(1) Å, P(1)−O(3) = 1.517(2) Å, P(1)−O(4) = 1.592(2) Å; P(2)−O(4) = 1.618(3) Å, P(2)−O(5) = 1.521(2) Å, P(2)−O(6) = 1.501(2) Å, P(2)−O(7) = 1.502(2) Å.)

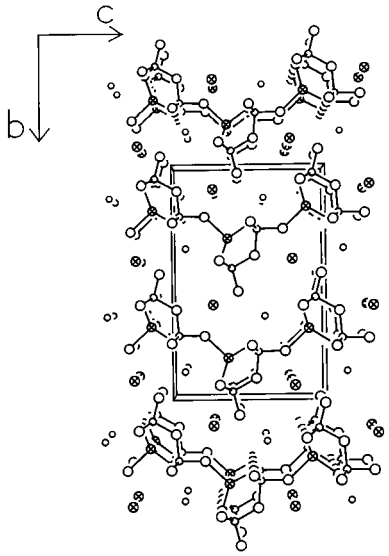

Figure 3. Perspective view of $NaCsMnP_2O_7$ along the *a* axis. The unit cell is outlined. The large crosshatched and small open circles represent Mn and P, respectively. The unbounded open and crosshatched circles are Na and Cs, respectively.

arranged along the *c* axis to form an undulating $[MnP_2O_7]_\infty$ ribbon. The electropositive cations, Na^+ and Cs^+, reside between the slabs of parallel ribbons. The ribbons, as shown in Figure 4, are interconnected through corner-sharing of MnO_5 and P_2O_7 units to form a Mn−P−O slab along the *ab* plane. Each P_2O_7 group links to three Mn atoms, and three MnO_5 polyhedra and three PO_4 tetrahedra share vertexes to form a ring. Mn atoms are 5-coordinate with the Mn−O bond distances varying between 1.99 and 2.17 Å, which are comparable to 2.20 Å, the corresponding bond distances observed in $K_2MnP_2O_7$.[9] In $K_2CuP_2O_7$,[5c] the Cu−O bond corresponding to the apical oxygen, O(6) in the present case, has a long distance of 2.36

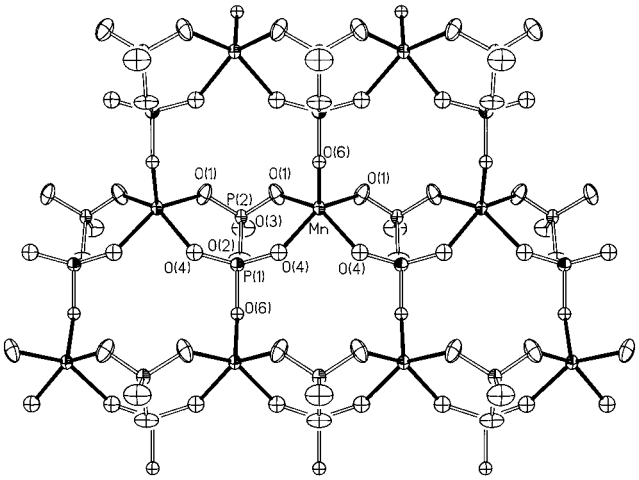

Figure 4. Partial structure of the $[MnP_2O_7]^{2-}$ slab in $NaCsMnP_2O_7$. The Mn−O and P−O bonds are indicated by solid and hollow lines, respectively. The anisotropic thermal ellipsoids are drawn at 70% probability. (Mn−O(1) = 2.100(4) Å × 2, Mn−O(4) = 2.158(9) Å × 2, Mn−O(6) = 1.992(18) Å; P(1)−O(2) = 1.622(6) Å, P(1)−O(4) = 1.483(9) Å × 2, P(1)−O(6) = 1.596(18) Å; P(2)−O(1) = 1.516(5) Å × 2, P(2)−O(2) = 1.629(6) Å, P(2)−O(3) = 1.483(6) Å.) For clarity, the disordered O(5) and O(7) atoms were omitted (Mn−O(5) = 2.172(10) Å, Mn−O(7) = 2.064(14) Å; P(1)−O(5) = 1.527(10) Å, P(1)−O(7) = 1.461(14) Å).

Å, which is much longer than the other four (1.94−1.98 Å) as might be expected for d^9 Cu^{2+}.

Both **2** and **3** exhibit disorder in their structural solutions. In **2**, O(4) and O(5) are a disordered pair as well as O(6) and O(7). The refined occupancies are 0.57/0.43 and 0.40/0.30 (×2), respectively, and the distances between the disordered oxygen atoms are 0.62 and 0.58 Å. In **3**, O(3) is disordered around a 2-fold axis, and the occupancy is reduced to 50% to compensate for the doubled multiplicity. In addition, the Mn and Cu atoms are statistically distributed at the same site, and the refined occupancies are 0.35(1) and 0.65(1), respectively. The bond valence sum calculations indicate that the formal oxidation state of manganese is Mn^{2+}.[20]

The IR spectra of **1** and **2** (Figure 5) are similar, as expected for these two compounds, which contain the same pyrophosphate groups. The peaks at 702.6/947.9 cm^{-1} for **1** and at 740.9/908.8 cm^{-1} for **2** are attributed to symmetric (ν_s) vs asymmetric (ν_{as}) P−O−P vibrations. The difference in the P−O−P angles, 145.8(2) vs 124.8(4)°, respectively, may be responsible for the blue shift of ν_s and red shift of ν_{as}. The corresponding peaks for $K_2CuP_2O_7$ are located at 705/908 cm^{-1}.[5b] The O−P−O bending and P−O stretching vibrational frequencies associated with the PO_4 groups are shown as multiple bands in the ranges 400−680 and 1000−1300 cm^{-1}, respectively.

The electropositive cations reside in the gaps between the stacked slabs. There are two types of Na^+ atoms in **1**: one surrounded by seven oxygen atoms with Na−O distance ranging from 2.28 to 2.93 Å; the other surrounded by eight oxygen atoms with distances ranging from 2.43 to 2.81 Å. In **2**, the Na^+ and Cs^+ cations adopt 5-coordination (2.26−2.99 Å) and 12-coordination (3.07−3.64 Å), respectively. In **3**, these cations are 6-coordinate (2.27−2.89 Å) and 9-coordinate (3.14−3.39 Å), respectively.

(20) (a) Brown, I. D.; Altermatt, D. *Acta Crystallogr.* **1985**, *B41*, 244. (b) Brese, N. E.; O'Keefe, M. *Acta Crystallogr.* **1991**, *B47*, 192. (c) Results of bond valence sum calculations for all the cations (in parentheses): 1.03/0.91 (Na^+), 2.09 (Mn^{2+}), 4.87/4.85 (P^{5+}) for **1**; 0.98 (Na^+), 0.97 (Cs^+), 2.11 (Mn^{2+}), 4.90/4.86 (P^{5+}) for **2**; 0.99 (Na^+), 0.91 (Cs^+), 2.10 (Mn^{2+}/Cu^{2+}), 5.22/4.85 (P^{5+}) for **3**.

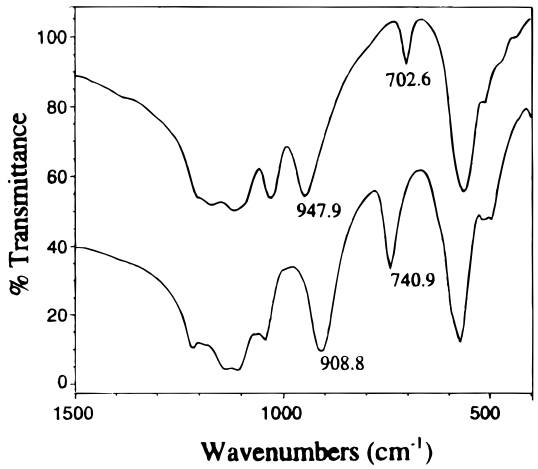

Figure 5. Infrared spectra of $Na_2MnP_2O_7$ (top) and $NaCsMnP_2O_7$ (bottom).

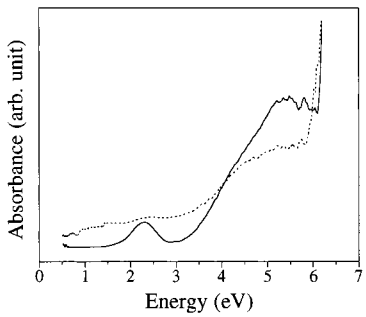

Figure 6. UV−vis spectra of $Na_2MnP_2O_7$ (dotted line) and $NaCsMnP_2O_7$ (solid line).

The UV−vis spectra of $Na_2MnP_2O_7$ and $NaCsMnP_2O_7$ (Figure 6) are consistent with the local geometry and the coordination of the divalent manganese cation. $Na_2MnP_2O_7$ is colorless, and its absorption spectrum is transparent in the visible region. The corresponding Mn^{2+} cation adopts a distorted octahedral geometry, and the d−d transition of a high-spin d^5 electron configuration is forbidden. $NaCsMnP_2O_7$, however, is purple and exhibits an absorption peak at ∼2.3 eV (539 nm). This absorption is likely a result of the square pyramidal distortion.

As portrayed in Figure 7a, the plot of χ^{-1} (inverse molar susceptibility) versus T (temperature) shows that $Na_2MnP_2O_7$ obeys the ideal Curie−Weiss type paramagnetic behavior over the range 10−300 K and undergoes an antiferromagnetic ordering at about 7.2 K (see inset). The paramagnetic data were fitted to the Curie−Weiss equation, $\chi = \chi_0 + C/(T - \Theta)$, where χ_0 is the temperature-independent paramagnetism, C is the Curie constant, and Θ is the Weiss constant. The model yielded best-fit values of $\chi_0 = 9.60 \times 10^{-4}$ emu/mol, $C = 4.02$ emu·K/mol, and $\Theta = -9.02$ K, corresponding to a μ_{eff} of 5.70 μ_B, which is slightly lower than the ideal value of 5.92 μ_B for a single manganese(II), high-spin d^5.

Remarkably, there is no noticeable deviation from the Curie−Weiss law which would be expected if significant short-range correlations were present. In the present example, one expects a broad susceptibility maximum for the Mn_2O_{10} dimers due to the short-range order in contrast to the sharp maximum seen at 7.2 K (Figure 7a). This sharp transition is similarly seen in the reported susceptibility data of $Fe_2As_4O_6$,[21] whose structure exhibits isolated $Fe_2O_9^{12-}$ dimers. According to Nakua and Greedan,[21] the reason for the absence of any significant dimer-like short-range order in the magnetic susceptibility is 2-fold. First, the bridging angle of the dimeric unit is abruptly different from 180°, Mn−O(1)−Mn = 99.1° in this case, which will cause the magnitude of the spin interaction to be very small, and this will result in a weaker intradimer interaction.[22] Second, the interdimer interactions via other superexchange pathways outnumber the intradimer exchange interactions and hence their sum can overwhelm the intradimer interaction. The possible interdimer exchange pathways are said to be via oxyanions, PO_4 tetrahedra in this case.

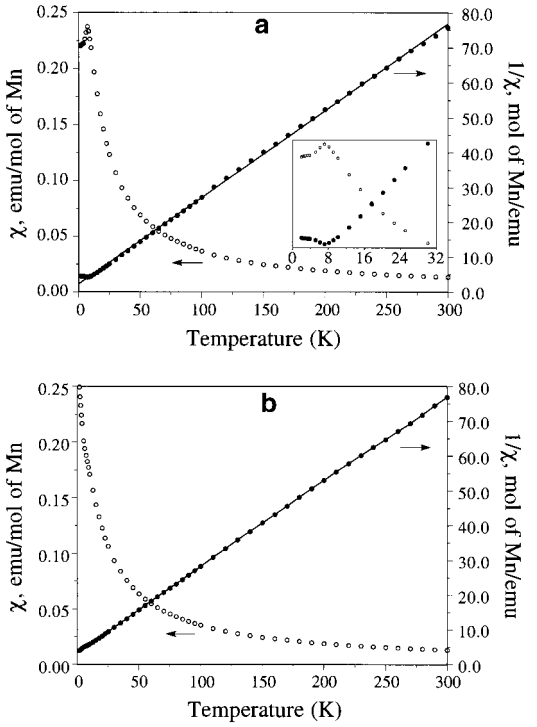

Figure 7. Magnetic susceptibility of (a) $Na_2MnP_2O_7$ and (b) $NaCsMnP_2O_7$.

Figure 7b shows the χ and χ^{-1} versus T plots of $NaCsMnP_2O_7$ indicating that the compound contains isolated magnetic ions with no significant long-range magnetic ordering. The χ^{-1} versus T plot obeys the ideal Curie−Weiss type paramagnetic behavior over almost the entire temperature range, 1.78−300 K. The paramagnetic data were fitted to the Curie−Weiss equation stated above. The model yielded best-fit values of $\chi_0 = 3.48 \times 10^{-5}$ emu/mol, $C = 4.07$ emu·K/mol, and $\Theta = -14.45$ K, corresponding to a μ_{eff} of 5.73 μ_B, close to the spin-only value of 5.92 μ_B for d^5.

In summary, three new layered compounds, $Na_2MnP_2O_7$, $NaCsMnP_2O_7$, and $NaCsMn_{0.35}Cu_{0.65}P_2O_7$, have been isolated by high-temperature, solid-state methods. $Na_2MnP_2O_7$ adopts a new structure type that contains a novel cage unit made of two Mn_2O_{10} dimers and two P_2O_7 groups. Despite the complexity of the mixed framework, it is recognized that the structurally isolated TM−oxide frameworks, dimeric Mn_2O_{10} and monomeric MnO_5, are electronically confined, that is to say that the Mn^{2+} d electrons are localized and the manganese oxide units behave like discrete molecules. These differently sized TM−oxide frameworks can be obtained by incorporating different A-site cations, and parameters describing the correlation between the incorporated A-site cation and shape and size of the TM−

(21) Nakua, A. M.; Greedan, J. E. *Inorg. Chem.* **1995**, *34*, 1373.

(22) Hay, P. J.; Thibeault, J. C.; Hoffmann, R. *J. Am. Chem. Soc.* **1975**, *97*, 4884.

oxide lattice need to be further investigated. To complete the study of the $A_2MnP_2O_7$ series, it would be interesting to see what structures $(Li,Cs)_2MnP_2O_7$ adopt.

Acknowledgment. Financial support for this research (Grant DMR-9612148) and the single-crystal X-ray diffractometer from the National Science Foundation is acknowledged.

Supporting Information Available: Tables of detailed crystallographic data, anisotropic thermal parameters, and bond distances and angles for **1**−**3** (9 pages). Ordering information is given on any current masthead page.

IC980616D